Version of Record: https://www.sciencedirect.com/science/article/pii/S2451929423005600
Manuscript_a7024d2098019c48dd35ca76d6cc3530

A Butadiene-Derived Semicrystalline Polyolefin with Two-Tiered Chemical Recyclability

Authors: Cherish Nie,[1,6] Shawn M. Maguire,[2,6] Callie W. Zheng,[2] Megan Mohadjer Beromi,[3] Richard A. Register,[3,4] Rodney D. Priestley,[3,4] Emily C. Davidson,[3,4,*] Paul J. Chirik[1,5,**]

[1]Department of Chemistry, Princeton University, Princeton, NJ, 08540
[2]Department of Chemical and Biological Engineering, Princeton University, Princeton, NJ, 08544
[3]Department of Chemistry, United States Naval Academy, Annapolis, MD, 21402
[4]Princeton Materials Institute, Princeton University, Princeton, NJ, 08540
[5]Lead contact
[6]These authors contributed equally
*Correspondence: edavidson@princeton.edu
**Correspondence: pchirik@princeton.edu

SUMMARY: Commodity polyolefins account for the majority of plastic waste but are challenging to depolymerize or upcycle due to the high thermal and chemical stability of hydrocarbon polymer backbones. Herein, we report a class of polyolefin that undergoes clean and selective chemical recycling at both the oligomeric and polymeric stages. [2+2] cycloaddition of the monomer butadiene formed telechelic oligomers (1,*n*′-divinyl)oligocyclobutane (DVOCB) that undergo deoligomerization back to butadiene. From the oligomer DVOCB, chain extension using acyclic diene metathesis (ADMET) yielded the polyolefin pDVOCB. Reverse ADMET of pDVOCB enabled full recovery of the telechelic oligomer. pDVOCB polymers are semicrystalline hydrocarbon polymers with high melting temperatures (T_m > 230°C) that have excellent chemical and hydrolytic stability and comparable mechanical properties to commodity polyolefins such as polypropylene and polyethylene. Thus, this work demonstrates a class of semicrystalline polyolefins capable of two tiers of chemical recycling.

KEY WORDS: closed-loop, chemical recycling, polyolefin, butadiene, ADMET

INTRODUCTION

Polyolefins account for more than 60% of global plastics production and are among the most ubiquitous consumer materials.[1] Their favorable characteristics include robust thermomechanical properties, chemical inertness, and sourcing from abundant feedstock olefins which translates to low cost.[1] These same qualities present barriers to efficient recycling and are also responsible for the accumulation of polyolefins in landfills and the environment.[1,2,3] Chemical recycling is gaining increased attention for its potential to depolymerize polymers directly to constituent monomers that can be repolymerized into virgin-quality materials or upcycled by chemical modification to value-added products. Such an approach turns plastic waste into a valuable resource and is a key step toward achieving a circular plastics economy.[4,5] However, achieving the chemical recycling of commodity polyolefins such as polyethylene (PE) and polypropylene (PP), which were not developed with end-of-life considerations in mind, is

challenging due to their thermodynamic stability.[4] This limitation motivates the development of next-generation polymer microstructures designed for closed-loop chemical recycling.[6]

Approaches to chemically recyclable polymers have relied on two primary strategies: (*i*) the incorporation of cleavable heteroatomic linkages in the polymer backbone, and (*ii*) the engineering of cyclic monomers with highly tailored ring strains (Figure 1A).[7] The strategic placement of cleavable groups or comonomers in the backbone of traditional polymers has been demonstrated to enable chemical recycling or upcycling while preserving material properties.[8–11] A variety of cyclic monomers—most commonly cyclic esters,[12–14] cyclic thioesters,[15–17] cyclic carbonates,[18] cyclic acetals,[19] and cyclic olefins[20]—have been designed to undergo reversible ring-opening polymerization under mild conditions. However, polymers with heteroatomic backbones struggle to retain the thermal and hydrolytic stability characteristic of traditional, fully hydrocarbon polyolefins while the use of specialized monomers cannot compete with the scale and availability of feedstock olefins. Among the novel polymer microstructures reported that are capable of chemical recycling to monomer, hydrocarbon-based polymers are much less developed compared to those with heteroatomic backbones,[21,22] and pure polyolefins are particularly rare. Olefin metathesis is an attractive strategy to synthesize recyclable polymers with hydrocarbon backbones as polymerization and depolymerization take place only in the presence of catalyst and the functional group, air, and water tolerance of ruthenium metathesis catalysts enables their application to a host of materials under a range of conditions.[23,24] For example, Wang and coworkers have reported a series of fused-ring cyclooctene monomers including *trans*-cyclobutane- and *trans*-cyclopentane-fused cyclooctene that exhibit fine-tuned ring strain, enabling reversible ring-opening metathesis polymerization (ROMP) under mild conditions (Figure 1B).[15,25] Recently, the groups of Chen[26] and Hong[27] have expanded the fused-ring strategy to cyclohexene derivatives. The resulting polymers feature excellent thermal stability and may have tunable properties through modifications of the fused-ring component, but thus far are limited to amorphous polymers and require multi-step monomer syntheses. There is a critical need to further expand the space of chemically recyclable hydrocarbon polymers, ideally prepared in minimal steps from feedstock monomers to make use of the preexisting infrastructure and resources that support commodity polyolefins.

Butadiene is a feedstock monomer that can be produced both by petrochemical[28] and bio-based routes[29,30] and serves as a building block for synthetic rubbers and a host of other applications. Chirik and coworkers have reported a unique, iron-catalyzed method for the [2+2] cyclo(oligomerization) of butadiene resulting in a 1,3-enchained cyclobutyl microstructure with telechelic vinyl end groups known as (1,*n*′-divinyl)-oligocyclobutane (DVOCB) (Figure 1C).[31,32,33] Notably, this microstructure was shown to undergo retro-[2+2] cycloaddition to regenerate butadiene, demonstrating the potential for chemical recycling. However, two major issues limit the development of DVOCB as a chemically recyclable polyolefin; the high crystallinity of DVOCB resulted in precipitation from the oligomerization reaction at low molecular weights (M_n < 1,000 g/mol) and the deoligomerization to butadiene was a time consuming and low yielding process. Alternative strategies to increase polymer chain length and improve the efficiency of chemical recycling are needed to achieve a truly chemically recyclable polyolefin. The terminal vinyl groups of DVOCB and its selective synthesis make it well suited as a monomer for acyclic diene metathesis (ADMET)[34] polymerization, where through olefin metathesis and loss of

ethylene, chain-extension of DVOCB to form a polyolefin, pDVOCB, is possible (Figure 1D). Unlike ROMP which is driven by monomer ring-strain and relies heavily on monomer design, ADMET is driven by removal of ethylene and is reversed by ethenolysis,[35] enabling the depolymerization of pDVOCB back to DVOCB. ADMET depolymerization has also been demonstrated in the conversion of conventional polymers such as 1,4-polybutadiene to precise telechelic oligomers.[36,37] More recently, it has been employed in the catalytic deconstruction of PE to propylene through a combination of dehydrogenation, ethenolysis, and isomerization.[38,39]

Here, we describe the synthesis, characterization, and properties of a chemically recyclable polyolefin microstructure derived from butadiene using reversible iron-catalyzed [2+2] cycloaddition-oligomerization in conjunction with ruthenium-catalyzed ADMET polymerization. pDVOCB is a semicrystalline material with high thermal stability (onset of degradation temperature, T_d = 365°C) and storage modulus comparable to semicrystalline commodity polyolefins such as isotactic PP (iPP) and high-density polyethylene (HDPE). Investigation into the structure-property relationships of pDVOCB established a dependence of the crystallinity on the chain length of the DVOCB subunit, allowing for easily tunable material properties without increasing synthetic complexity. Depolymerization of pDVOCB afforded pristine DVOCB with minimal purification, and repolymerization achieved both the molecular weight and physical properties of the virgin polymer. Furthermore, a scalable and efficient method for the deoligomerization of DVOCB back to pristine butadiene closes the loop between polymer and feedstock monomer.

RESULTS AND DISCUSSION

DVOCB Oligomer Synthesis and Thermal Properties. In the previously reported synthesis,[31] only a narrow range of DVOCB oligomers was prepared, consisting of mostly insoluble oligomers with poor control over average chain-length and little insight into the molecular weight distribution (MWD). To prepare soluble oligomers more amenable to polymerization and on larger scale, initial efforts were focused on the synthesis and characterization of short-chain ($n < 8$) DVOCB. Ideally, the developed method would reliably generate different average oligomer lengths to probe the effects of the value of n on the chain-extended polymer.

Experimental conditions for oligomerization using the iron precatalyst **((^{Me}EtPDI)FeN$_2$)$_2$(μ-N$_2$)** (^{Me}EtPDI = 2,6-(2,6-Me$_2$-C$_6$H$_3$-N=CEt)$_2$C$_5$H$_3$N)[40] were systematically explored to determine their effects on DVOCB length and yield. The most effective and reproducible method to target specific oligomer chain lengths was by moderating the reaction time using neat conditions with a catalyst loading of 0.075–0.1 mol %. Short-chain oligomers with n = 4–7 (12–45% yield) were successfully isolated with consistent yields that increased with average oligomer length (Figure 2). While the yield for oligomers was low to moderate per batch, unreacted butadiene was directly and repeatedly resubjected to reaction conditions without additional purification, resulting in a combined yield of up to 72% based on the initial charge of butadiene (Table S2). Additional butadiene may be added to replace the butadiene consumed per cycle, enabling continuous and consistent generation of the desired DVOCB(n). This process enabled the production of multi-gram quantities of short-chain oligomer sufficient for polymerization. The presence of solvents, change in catalyst loading, and reduced reaction temperatures did not improve chain length control or oligomer yield (Table S3). The tacticity of these short-chain oligomers is consistent with previous observations,[31]

that is an equal fraction of *syn* and *anti* cyclobutane rings and a preference for alternating cyclobutane dispositions along the chain. Current efforts in catalyst development are focused on generating exclusively short-chain oligomers to improve yield and stereoregular oligomers to modify polymer properties.

The values of n and M_n for each batch of oligomer were determined by end-group analysis using ^{1}H NMR spectroscopy. Because the molecular weights of these oligomers are too low to be reliably analyzed by gel-permeation chromatography (GPC), matrix assisted laser desorption ionization-time of flight (MALDI-TOF) mass spectrometry was used to measure the mass distribution of oligomers and to corroborate the average oligomer length obtained by ^{1}H NMR spectroscopy. MALDI-TOF analysis established reasonable agreement with the ^{1}H NMR measurements as well as consistency between independent batches of DVOCB of the same n. The oligomer distribution and dispersity (Đ) for each n is reflective of the isolated oligomer material and not representative of the distribution during oligomerization. Notably, the MWD is distinct (Figures S19–22) and narrow (Đ ≤ 1.05) for a given n (Figure 2).

The thermal behavior of short-chain DVOCB was investigated using thermogravimetric analysis (TGA, Figure 3A) and differential scanning calorimetry (DSC, Figure 3B). The insoluble oligomers DVOCB(10) and DVOCB(15) were prepared for comparison by the unmodified reported procedure.[31] The onset temperature of mass loss (T_d) for the shortest oligomer, DVOCB(4), is 175°C and increases to 290°C for the longest oligomer, DVOCB(15). For the shorter oligomers, volatilization may make a more significant contribution to initial mass loss than degradation. A second degradation event was observed around 416°C for all oligomer lengths that is attributed to the degradation of thermally crosslinked material.[41]

DSC of the DVOCB oligomers indicated that these materials are semicrystalline with the temperatures of thermal transitions and degree of crystallinity highly sensitive to the average number of cyclobutyl repeat units in the oligomer. Two endothermic transitions are evident upon heating (Figure 3B) which were previously attributed to a crystal-to-rotator phase transition (T_1) and a rotator phase-to-melting transition (T_m) in DVOCB(17) and have been corroborated by wide-angle X-ray scattering (WAXS) and additional DSC measurements.[31] A rotator phase refers to a phase wherein the crystal stems are rotationally disordered.[42,43] As n increases, the temperatures of all transitions also increase. This trend has been observed in alkanes, where the rotator phase transition temperatures are dependent on the molecular weight of the alkane.[44,45]

Polymer Synthesis and Thermomechanical Properties. ADMET polymerization was used as a strategy for chain extension to achieve high molecular weight polyolefin microstructures with enchained cyclobutyl units. Soluble, short-chain DVOCB(n) oligomers were subjected to solution ADMET conditions in xylene (or mesitylene) under a constant argon flow to drive ethylene removal. The semicrystallinity of the resulting polymer necessitated high temperatures (>100°C) to maintain a homogeneous solution and required the use of a high-temperature stable metathesis catalyst. A selection of ruthenium metathesis catalysts was evaluated (Table S8) for minimal tendency towards olefin isomerization and high activity. The commercially available cyclic alkylaminocarbene ruthenium metathesis catalyst **M1002** ($RuCl_2$(CAAC)(=CHAr); CAAC = (2,6-^{i}Pr$_2$-C_6H_3)-3,5,5-Me_3-3-Ph-pyrrolidin-2-ylidene, Ar = C_6H_4-2-O^{i}Pr), which has previously demonstrated utility in high temperature bulk ADMET reactions,[46] best fit

the desired criteria. A small quantity of benzoquinone (BQ) was also added to each polymerization to suppress olefin isomerization, a known strategy for minimizing this common side-reaction during ruthenium-catalyzed metathesis reactions, particularly at elevated temperatures.[47,48] Polymers prepared using this ADMET procedure are denoted as pDVOCB(n, m) (m = average number of enchained DVOCB(n)) and were obtained as off-white powders in good yield.

Like PE and PP, these chain-extended polymers are insoluble in common organic solvents at room and moderate temperatures in line with the chemical stability typical of polyolefins, but this presents a major challenge for molecular weight characterization, precluding many common techniques used to study polymer molecular weight distribution such as conventional GPC and MALDI-TOF mass spectrometry. Solvent-free sample preparation was attempted for MALDI-TOF analysis but was unsuccessful. Instead, characterization of pDVOCB relied on techniques with high-temperature capabilities. Number-average molecular weights (M_n) and degree of polymerization m were determined by end-group analysis with high-temperature ^{1}H NMR spectroscopy in 1,1,2,2-tetrachloroethane-d_2 (TCE-d_2) at 140°C, which resolved and differentiated the emergent internal alkene protons between 5.25–5.28 ppm from the terminal vinyl protons at 5.01 ppm and between 5.93–6.15 ppm. Weight-average molecular weights (M_w) and dispersities were determined by high-temperature GPC (HT-GPC) in 1,2,4-trichlorobenzene (TCB) at 145°C (Figure 4). The values of M_n from endgroup analysis by ^{1}H NMR spectroscopy are consistently higher than the values of M_w/Đ from HT-GPC which may be due (at least in part) to the difference in hydrodynamic volume between pDVOCB and the linear polyethylene used for calibration. Nevertheless, this range of molecular weights was sufficient for initial studies.

To probe the structure-property relationships of these unique olefin-spaced enchained cyclobutyl architectures, ADMET polymerizations were carried out with DVOCB(4–10). A positive correlation was observed between n and the temperature required to maintain a completely soluble reaction mixture, suggesting that polymer melting temperature is dependent on average oligomer length n (Figure 4).[49] This trend was corroborated by thermal analysis (*vide infra*). A steep decrease in the degree of polymerization and increase in the amount of end-group isomerization were also observed for $n \geq 7$, which were attributed to the increasing melting temperature (hence insolubility) of the forming polymer as well as increased rates of catalyst decomposition and end-group isomerization at the most elevated temperatures.

TGA was performed to determine the role of both oligomer length n and degree of polymerization m on the thermal degradation behavior of the resulting polymer. Upon chain-extension from DVOCB(n) to pDVOCB(n, m), the initial onset T_d was around 365°C for all polymers examined (Figure 5A), demonstrating excellent thermal stability. Using a TGA coupled with a mass spectrometer (TGA-MS) under identical operational conditions, the evolved gas from the polymer samples was analyzed during heating. MS (EI+) analysis indicated that the volatiles formed during the initial mass loss were composed of one major component, divinylcyclobutane (Figure S42). Thermo-oxidation of commodity polyolefins and their derivatives is common and has been reported with PS, PE, and PP.[50] TGA in air revealed an onset of oxidation at 240°C for pDVOCB(n, m) polymers (Figures S38 and S39). The reduced stability of pDVOCB(n, m) in oxygen-rich environments is comparable to iPP which also contains

tertiary carbon centers and exhibits oxidative degradation at 255°C, while HDPE undergoes oxidative degradation at a higher temperature of 375°C (Figures S36 and S37).

DSC was performed on a series of pDVOCB(*n, m*) polymers to further investigate the effects of constituent DVOCB(*n*) on thermal properties (Figure 5B). Multiple endothermic events and highly crystalline behavior were observed that persisted over multiple heating and cooling cycles (Figure S48). All endothermic peaks shift to higher temperatures as *n* is increased across the series, with the melting temperature shifting from 238°C to 258°C and crystallization temperatures shifting from 214°C to 237°C. This trend indicates that *n* has a major role in dictating the melting temperature of the resultant polymer. For all synthesized pDVOCB polymers, the melting temperature is much higher than that of iPP (T_m = 165°C) and HDPE (T_m = 135°C) (Figure S49), demonstrating the possibility for pDVOCB to be used in high-temperature applications. Additionally, temperature-modulated DSC analysis did not reveal an observable glass transition (T_g) for pDVOCB(*n, m*) polymers within the investigated temperature range of –80°C to 275°C (Figure S52).

Based on the thermal behavior of DVOCB, the minor endothermic transitions T_1 and T_2 of pDVOCB polymers may arise from the solid crystal fraction transitioning to a rotator phase before reaching the melting temperature. To test this, variable-temperature WAXS was performed on DVOCB(10) and pDVOCB(6, 42), revealing the appearance of a rotator phase upon heating to temperatures $T_1 < T < T_m$ for both samples (Figure 6), suggesting similar temperature-dependent ordering of DVOCB oligomers and pDVOCB polymers. For pDVOCB(6, 42), a single rotator-phase transition is observed by WAXS, in contrast to the two endotherms observed by DSC (Figure 5B) which is under ongoing investigation. The observation of multiple endothermic events is typical for semicrystalline materials (e.g. poly(L-lactic acid), poly(ethylene terephthalate)) and is likely indicative of other crystallization phenomena such as secondary crystallization, crystal lamellar perfection/thickening, and melting-recrystallization which may be occurring simultaneously.[51-54]

The mechanical properties of the pDVOCB(*n, m*) were investigated by dynamic mechanical analysis (DMA) and tensile testing. Rectangular bars of pDVOCB and commercial HDPE (M_w = 66 kg/mol) and iPP (M_w = 243 kg/mol) were prepared by melt-pressing in air to simulate real-world processing conditions (Figure S2). Due to concerns of thermo-oxidation, TGA, DSC, and attenuated total reflection infrared (ATR-IR) spectroscopy were used to evaluate the processed bars and revealed negligible oxidation under appropriate processing conditions (see Supplemental Information). Using a single-cantilever setup, DMA showed that pDVOCB(5,40) possesses a relatively high storage modulus (E′) at room temperature followed by a continuous decrease until reaching the beginning of viscous flow at 175°C (Figure 7A). The peak in tan δ around 140°C is ascribed to the rotator-phase transition evident in DSC and WAXS which imparts partial chain mobility and allows for energy dissipation. Because mechanical measurements such as by DMA are often more sensitive to chain relaxations than DSC to changes in heat capacity,[55] a glass transition (defined as the peak maxima in tan δ) was detectable by DMA at 50°C which was more definitively confirmed by sub-ambient DMA (Figure S57). Overall, the storage modulus of pDVOCB(5,40) was comparable to that of HDPE and iPP and also maintained rigidity up to significantly higher temperatures. Under tensile testing (Figures S60–65), the average strain at break of pDVOCB(5,40) was 7% which is comparable to that of iPP at 10% while HDPE exhibited a higher average strain at break of 177%. While these

values are indicative of brittle materials, pDVOCB(5, 67) exhibited an average strain at break of 42% which was six times higher than that of pDVOCB(5,40), suggesting that optimizing polymerization conditions to achieve higher molecular weight polymers improves ductility (Figure 7B). For example, at much higher relative molecular weights, melt-pressed bars of HDPE (M_w = 125 kg/mol) and iPP (M_w = 550 kg/mol) exhibited average breaking strains of 1,430% and 870%, respectively (Figure 7C).

Solvent resistance was also evaluated to gain insight into potential applications. Melt-pressed bars of pDVOCB(6, 42) and pDVOCB(5, 40) demonstrated excellent stability when subjected to dissolution tests in a range of solvents as well as in aqueous acidic and basic conditions for up to six weeks at room temperature and elevated temperatures which is consistent with the behavior of polyolefins (Figure S67).

Chemical Recycling of pDVOCB and DVOCB. The feasibility of depolymerization of pDVOCB by reverse ADMET was investigated using a representative polymer, pDVOCB(5, 43), in a series of optimization reactions (Table S7). Complete depolymerization and quantitative recovery of DVOCB was achieved by exposing the polymer to 1 mol % M1002, 5 mol % BQ, and 20 equivalents of ethylene (relative to DVOCB) in toluene (10 mg/mL) with a temperature ramp from 115°C to 50°C over the course of 24 hours (Figure 8A). The temperature gradient was used to improve ethylene solubility while maintaining polymer solubility at partial depolymerization. By end-group analysis using high temperature ^{1}H NMR spectroscopy, the average number of internal alkenes per polymer chain was reduced from 42 to 0.05, corresponding to >99% depolymerization. The oligomer was recovered in >99% yield through straightforward extraction with hexanes and filtration through a pad of silica to remove catalyst residue and BQ. The recycled DVOCB(5) (*r*-DVOCB(5)) was usable without further purification. Varying the equivalents of ethylene or diluting the reaction did not drastically affect the degree of depolymerization with all entries achieving at least 98% depolymerization. During the optimization phase, depolymerization reactions were conducted for 24 hours to ensure complete conversion, but >99% depolymerization and 96% yield were still maintained even at a reduced reaction time of 3 hours. Overall, the depolymerization of pDVOCB was shown to be a clean and robust process.

To demonstrate that pDVOCB polymers are amenable to chemical recycling, *r*-DVOCB(5) was subjected to ADMET polymerization conditions to yield the recycled polymer *r*-pDVOCB(5, 52) (Figure 8B). While the recycled oligomer was subjected to identical ADMET conditions, the recycled polymer had an 18% higher M_n that is attributed to experimental variations such as the effectiveness of ethylene removal, stirring speed, solution viscosity, and amount of solvent loss that are difficult to control precisely under laboratory conditions. To evaluate the scalability of this process, ADMET depolymerization was conducted on 1.0 g of pDVOCB(5, 67) and *r*-DVOCB(5) was isolated in 74% yield. The thermal properties of virgin and recycled pDVOCB (Figure 8C) and virgin and recycled DVOCB (Figures S44 and S56) were compared by TGA and DSC and showed no deterioration of thermal properties for the chemically recycled material.

To simulate more realistic recycling conditions, the chemical recycling of pDVOCB was also conducted from a mixed polymer feedstock. Postconsumer items made from PE, PP, and polystyrene, were collected, including facemasks, single-use food containers, sealable sandwich bags, and various lids and caps. These items—containing

pigments, stabilizers, plasticizers, and/or other additives—were added to a depolymerization reaction with pDVOCB(5, 67). Under the standard depolymerization conditions, *r*-DVOCB(5) was recovered in 90% yield and >99% depolymerization, with only minor alkane impurities carried over from the mixed plastic waste that do not interfere with repolymerization (Figure 8D), demonstrating that pDVOCB was chemically recycled from a mixture of commodity polyolefins without the need for specialized separation processes.

Having depolymerized pDVOCB to DVOCB, efforts were then directed towards the deoligomerization of DVOCB to butadiene to establish a complete and selective chemical recycling pathway from pDVOCB to feedstock olefin. Although the catalytic deoligomerization of short-chain soluble DVOCB to butadiene by retro-[2+2] cycloaddition was previously reported as a proof-of-concept,[31] the low yield of recovered butadiene (34%) and long reaction time of 6 days limited its practicality. Consequently, an improved and scalable method for the chemical recycling of DVOCB to butadiene was pursued.

The inefficient deoligomerization was primarily attributed to inhibition of the iron catalyst by the free butadiene generated by the reaction, slowing retro-[2+2] cycloaddition. To overcome this complication, many strategies were explored to remove free butadiene from the reaction to further drive deoligomerization while still maintaining a closed system such that butadiene could be recovered and quantified. An experimental design (Figure S1) using liquid nitrogen to trap evolving butadiene was the most effective, although trapping agents such as molecular sieves and N-methylpyrrolidone were also tried. The continuous removal of butadiene has additional benefits in that it enables access to higher temperatures, favoring deoligomerization without a dangerous buildup of pressure, and is amenable to any scale. With this design, the efficacy of deoligomerization was optimized using DVOCB(6) in mesitylene with 2.5 mol % ((^{Me}EtPDI)$FeN_2)_2(\mu\text{-}N_2$) (Figure 9). At 90°C, 76% yield of volatile products was generated consisting of butadiene (63%) and its [2+2] cycloaddition dimer 1,3-divinylcyclobutane (13%) after only 16 hours. Applying this improved method to *r*-DVOCB(5) and extending the reaction time to 24 hours enabled complete deoligomerization to butadiene (79%) and 1,3-divinylcyclobutane (21%) which, combined, represent >99% yield of volatile products. This result constitutes a significant improvement in the efficiency of catalytic deoligomerization and demonstrates that the inhibitory effects of coordination by free butadiene are overcome through process design.

It is worth noting that while pDVOCB has been selectively reverted to butadiene, for closed-loop recycling purposes it may actually be more preferable and practical to retain the oligomer as a solid and safer material for handling, transport, and repolymerization as compared to butadiene which is a toxic, gaseous reagent that is prone to spontaneous side reactions such as autopolymerization and spontaneous Diels-Alder dimerization.[56] However, for the purposes of upcycling and other applications, full feedstock recovery is an accessible option.

CONCLUSION

The combination of iron-catalyzed [2+2] cycloaddition-oligomerization and ruthenium-catalyzed ADMET polymerization has been applied to the synthesis of a family of alkene-spaced poly(oligocyclobutyl) polymers derived from butadiene, a commodity hydrocarbon monomer. The resulting materials are rare examples of polyolefins constructed exclusively from a commodity hydrocarbon feedstock that are amenable to closed-loop

chemical recycling between polymer and oligomer and between oligomer and monomer under relatively mild conditions. Variation in oligomer length also provided a straightforward method to tune polymer properties. These unique polymer microstructures demonstrated recyclability while retaining their thermomechanical properties and could be fully and selectively depolymerized from mixed polyolefin waste containing various colorants and additives, demonstrating the feasibility of chemical recycling in realistic conditions. pDVOCB exhibits excellent thermal stability (T_d = 365°C), and promising mechanical properties compared to commodity polyolefins such as iPP and HDPE. Future efforts will focus on the preparation of stereoregular (iso- and syndiotactic) DVOCB oligomers and the exploration of various polymer backbone modifications (*cis/trans* ratio and copolymerization) to further improve material properties.

EXPERIMENTAL PROCEDURES

Resource Availability

Lead Contact

Further information and requests for resources should be directed to and will be fulfilled by the Lead Contact, Paul J. Chirik (pchirik@princeton.edu).

Materials Availability

All unique materials generated in this study are available from the Lead Contact without restriction.

Data and Code Availability

All datasets generated within these investigations are available in the Supplemental Information.

ACKNOWLEDGMENTS

This research was supported by the U.S. Department of Energy, Office of Science, Office of Basic Energy Sciences, Catalysis Science program, under Award DE-SC0022303. C.W.Z. acknowledges funding from the High Meadows Environmental Institute (HMEI) Internship Program at Princeton. The authors acknowledge the use of Princeton's Imaging and Analysis Center (IAC) for DMA and TGA-MS analysis conducted in this work. The IAC is partially supported through the Princeton Center for Complex Materials (PCCM), a National Science Foundation (NSF)-MRSEC program (DMR-2011750). S.M.M. thanks Yejoon Seo and Nicholas J. Caggiano for DSC guidance, and C.N. thanks Dr. István Pelczer and Kenneth Conover for assistance with NMR spectroscopy and Saw Kyin for assistance with MALDI-TOF MS. The authors thank Dr. Coralie Duchemin for preparing the DVOCB(10) used in this work. The authors also thank Umicore for generously providing metathesis catalysts M1002, M1001, M800, and M801. Additionally, the authors thank Dr. Michael A. Webb for helpful discussions.

AUTHOR CONTRIBUTIONS

C.N. and S.M.M. carried out all experiments in this work and analyzed the data. C.W.Z. assisted in polymer characterization. M.M.B. conceptualized the idea and carried out initial experiments. P.J.C., E.C.D., R.A.R., and R.D.P. supervised the work and assisted in experimental design and data analysis. All authors contributed intellectually to the manuscript, and it was written and edited through contributions of all authors as well. All authors have given approval to the final version of the manuscript.

DECLARATION OF INTERESTS

The authors declare no competing interests.

REFERENCES

[1] Geyer, R., Jambeck, J.R., and Law, K.L. (2017). Production, use, and fate of all plastics ever made. Sci. Adv. *3*, e1700782. 10.1126/sciadv.1700782.

[2] Sardon, H., and Dove, A.P. (2018). Plastics recycling with a difference. Science *360*, 380–381. 10.1126/science.aat4997.

[3] Seeley, M.E., Song, B., Passie, R., and Hale, R.C. (2020). Microplastics affect sedimentary microbial communities and nitrogen cycling. Nat. Commun. *11*, 2372. 10.1038/s41467-020-16235-3.

[4] Coates, G.W., and Getzler, Y.D.Y.L. (2020). Chemical recycling to monomer for an ideal, circular polymer economy. Nat. Rev. Mater. *5*, 501–516. 10.1038/s41578-020-0190-4.

[5] Hong, M., and Chen, E.Y.-X. (2017). Chemically recyclable polymers: A circular economy approach to sustainability. Green Chem. *19*, 3692–3706. 10.1039/C7GC01496A.

[6] García, J.M. (2016). Catalyst: Design challenges for the future of plastics recycling. Chem *1*, 813–815. 10.1016/j.chempr.2016.11.003.

[7] Shi, C., Reilly, L.T., and Chen, E.Y.-X. (2023). Hybrid monomer design synergizing property trade-offs in developing polymers for circularity and performance. Angew. Chem. Int. Ed. *62*, e202301850. 10.1002/anie.202301850.

[8] Arroyave, A., Cui, S., Lopez, J.C., Kocen, A.L., LaPointe, A.M., Delferro, M., and Coates, G.W. (2022). Catalytic chemical recycling of post-consumer polyethylene. J. Am. Chem. Soc. *144*, 23280–23285. 10.1021/jacs.2c11949.

[9] Kocen, A.L., Cui, S., Lin, T.-W., LaPointe, A.M., and Coates, G.W. (2022). Chemically recyclable ester-linked polypropylene. J. Am. Chem. Soc. *144*, 12613–12618. 10.1021/jacs.2c04499.

[10] Kiel, G.R., Lundberg, D.J., Prince, E., Husted, K.E.L., Johnson, A.M., Lensch, V., Li, S., Shieh, P., and Johnson, J.A. (2022). Cleavable comonomers for chemically recyclable polystyrene: a general approach to vinyl polymer circularity. J. Am. Chem. Soc. *144*, 12979–12988. 10.1021/jacs.2c05374.

[11] Häußler, M., Eck, M., Rothauer, D., and Mecking, S. (2021). Closed-loop recycling of polyethylene-like materials. Nature *590*, 423–427. 10.1038/s41586-020-03149-9.

[12] Shi, C., Li, Z.-C., Caporaso, L., Cavallo, L., Falivene, L., and Chen, E.Y.-X. (2021). Hybrid monomer design for unifying conflicting polymerizability, recyclability, and performance properties. Chem *7*, 670–685. 10.1016/j.chempr.2021.02.003.

[13] Rapagnani, R.M., Dunscomb, R.J., Fresh, A.A., and Tonks, I.A. (2022). Tunable and recyclable polyesters from CO2 and butadiene. Nat. Chem. *14*, 877–883. 10.1038/s41557-022-00969-2.

[14] Li, X.-L., Clarke, R.W., Jiang, J.-Y., Xu, T.-Q., and Chen, E.Y.-X. (2022). A circular polyester platform based on simple gem-disubstituted valerolactones. Nat. Chem., 1–8. 10.1038/s41557-022-01077-x.

[15] Wang, Y., Li, M., Wang, S., Tao, Y., and Wang, X. (2021). S-Carboxyanhydrides: Ultrafast and selective ring-opening polymerizations towards well-defined functionalized polythioesters. Angew. Chem. Int. Ed. *60*, 10798–10805. 10.1002/anie.202016228.

[16] Zhu, Y., Li, M., Wang, Y., Wang, X., and Tao, Y. (2023). Performance-advantaged stereoregular recyclable plastics enabled by aluminum-catalytic ring-opening polymerization of dithiolactone. Angew. Chem. Int. Ed. *62*, e202302898. 10.1002/anie.202302898.

[17] Wang, Y., Zhu, Y., Lv, W., Wang, X., and Tao, Y. (2023). Tough while recyclable plastics enabled by monothiodilactone monomers. J. Am. Chem. Soc. 10.1021/jacs.2c11502.

[18] Saxon, D.J., Gormong, E.A., Shah, V.M., and Reineke, T.M. (2021). Rapid synthesis of chemically recyclable polycarbonates from renewable feedstocks. ACS Macro Lett. *10*, 98–103. 10.1021/acsmacrolett.0c00747.
[19] Abel, B.A., Snyder, R.L., and Coates, G.W. (2021). Chemically recyclable thermoplastics from reversible-deactivation polymerization of cyclic acetals. Science *373*, 783–789. 10.1126/science.abh0626.
[20] Sathe, D., Zhou, J., Chen, H., Su, H.-W., Xie, W., Hsu, T.-G., Schrage, B.R., Smith, T., Ziegler, C.J., and Wang, J. (2021). Olefin metathesis-based chemically recyclable polymers enabled by fused-ring monomers. Nat. Chem. *13*, 743–750. 10.1038/s41557-021-00748-5.
[21] Luo, X., Wei, Z., Seo, B., Hu, Q., Wang, X., Romo, J.A., Jain, M., Cakmak, M., Boudouris, B.W., Zhao, K., et al. (2022). Circularly recyclable polymers featuring topochemically weakened carbon–carbon bonds. J. Am. Chem. Soc. *144*, 16588–16597. 10.1021/jacs.2c06417.
[22] Song, Y., He, J., Zhang, Y., Gilsdorf, R.A., and Chen, E.Y.-X. (2022). Recyclable cyclic bio-based acrylic polymer via pairwise monomer enchainment by a trifunctional Lewis pair. Nat. Chem., 1–11. 10.1038/s41557-022-01097-7.
[23] Grubbs, R.H. (2004). Olefin metathesis. Tetrahedron *60*, 7117–7140. 10.1016/j.tet.2004.05.124.
[24] Ogba, O.M., Warner, N.C., O'Leary, D.J., and Grubbs, R.H. (2018). Recent advances in ruthenium-based olefin metathesis. Chem. Soc. Rev. *47*, 4510–4544. 10.1039/C8CS00027A.
[25] Zhou, J., Sathe, D., and Wang, J. (2022). Understanding the structure–polymerization thermodynamics relationships of fused-ring cyclooctenes for developing chemically recyclable polymers. J. Am. Chem. Soc. *144*, 928–934. 10.1021/jacs.1c11197.
[26] Shi, C., Clarke, R.W., McGraw, M.L., and Chen, E.Y.-X. (2022). Closing the "one monomer–two polymers–one monomer" loop via orthogonal (de)polymerization of a lactone/olefin hybrid. J. Am. Chem. Soc. *144*, 2264–2275. 10.1021/jacs.1c12278.
[27] Choi, K., and Hong, S.H. (2023). Chemically recyclable oxygen-protective polymers developed by ring-opening metathesis homopolymerization of cyclohexene derivatives. Chem. 10.1016/j.chempr.2023.05.038.
[28] White, Wm.C. (2007). Butadiene production process overview. Chem. Biol. Interact. *166*, 10–14. 10.1016/j.cbi.2007.01.009.
[29] Pomalaza, G., Ponton, P.A., Capron, M., and Dumeignil, F. (2020). Ethanol-to-butadiene: the reaction and its catalysts. Catal. Sci. Technol. *10*, 4860–4911. 10.1039/D0CY00784F.
[30] Kuznetsov, A., Kumar, G., Ardagh, M.A., Tsapatsis, M., Zhang, Q., and Dauenhauer, P.J. (2020). On the economics and process design of renewable butadiene from biomass-derived furfural. ACS Sustain. Chem. Eng. *8*, 3273–3282. 10.1021/acssuschemeng.9b06881.
[31] Mohadjer Beromi, M., Kennedy, C.R., Younker, J.M., Carpenter, A.E., Mattler, S.J., Throckmorton, J.A., and Chirik, P.J. (2021). Iron-catalysed synthesis and chemical recycling of telechelic 1,3-enchained oligocyclobutanes. Nat. Chem. *13*, 156–162. 10.1038/s41557-020-00614-w.
[32] Beromi, M.M., Younker, J.M., Zhong, H., Pabst, T.P., and Chirik, P.J. (2021). Catalyst design principles enabling intermolecular alkene-diene [2+2] cycloaddition and depolymerization reactions. J. Am. Chem. Soc. *143*, 17793–17805. 10.1021/jacs.1c08912.
[33] Kovel, C.B., Darmon, J.M., Stieber, S.C.E., Pombar, G., Pabst, T.P., Theis, B., Turner, Z.R., Üngör, Ö., Shatruk, M., DeBeer, S., et al. (2023). Bimolecular reductive elimination of ethane from pyridine(diimine) iron methyl complexes: mechanism, electronic structure, and entry into [2+2] cycloaddition catalysis. J. Am. Chem. Soc. *145*, 5061–5073. 10.1021/jacs.2c10547.
[34] Wagener, K.B., Boncella, J.M., and Nel, J.G. (1991). Acyclic diene metathesis (ADMET) polymerization. Macromolecules *24*, 2649–2657. 10.1021/ma00010a001.
[35] Davidson, T.A., and Wagener, K.B. (2013). Acyclic Diene Metathesis (ADMET) Polymerization. In Materials Science and Technology (John Wiley & Sons, Ltd). 10.1002/9783527603978.mst0226.
[36] Marmo, J.C., and Wagener, K.B. (1995). ADMET depolymerization. Synthesis of perfectly difunctional (f = 2.0) telechelic polybutadiene oligomers. Macromolecules *28*, 2602–2606. 10.1021/ma00112a002.
[37] Marmo, J.C., and Wagener, K.B. (1993). Acyclic diene metathesis (ADMET) depolymerization. Synthesis of mass-exact telechelic polybutadiene oligomers. Macromolecules *26*, 2137–2138. 10.1021/ma00060a051.
[38] Conk, R.J., Hanna, S., Shi, J.X., Yang, J., Ciccia, N.R., Qi, L., Bloomer, B.J., Heuvel, S., Wills, T., Su, J., et al. (2022). Catalytic deconstruction of waste polyethylene with ethylene to form propylene. Science *377*, 1561–1566. 10.1126/science.add1088.
[39] Wang, N.M., Strong, G., DaSilva, V., Gao, L., Huacuja, R., Konstantinov, I.A., Rosen, M.S., Nett, A.J., Ewart, S., Geyer, R., et al. (2022). Chemical recycling of polyethylene by tandem catalytic conversion to propylene. J. Am. Chem. Soc. *144*, 18526–18531. 10.1021/jacs.2c07781.

[40] Russell, S.K., Hoyt, J.M., Bart, S.C., Milsmann, C., Stieber, S.C.E., Semproni, S.P., DeBeer, S., and Chirik, P.J. (2014). Synthesis, electronic structure and reactivity of bis(imino)pyridine iron carbene complexes: evidence for a carbene radical. Chem. Sci. *5*, 1168–1174. 10.1039/C3SC52450G.
[41] Brazier, D.W., and Schwartz, N.V. (1978). The effect of heating rate on the thermal degradation of polybutadiene. J. Appl. Polym. Sci. *22*, 113–124. 10.1002/app.1978.070220109.
[42] Lee, L.-B.W., and Register, R.A. (2005). Hydrogenated ring-opened polynorbornene: A highly crystalline atactic polymer. Macromolecules *38*, 1216–1222. 10.1021/ma048013a.
[43] Sirota, E.B., King, H.E., Jr., Singer, D.M., and Shao, H.H. (1993). Rotator phases of the normal alkanes: An x-ray scattering study. J. Chem. Phys. *98*, 5809–5824. 10.1063/1.464874.
[44] Cholakova, D., and Denkov, N. (2019). Rotator phases in alkane systems: In bulk, surface layers and micro/nano-confinements. Adv. Colloid Interface Sci. *269*, 7–42. 10.1016/j.cis.2019.04.001.
[45] Sirota, E.B., and Singer, D.M. (1994). Phase transitions among the rotator phases of the normal alkanes. J. Chem. Phys. *101*, 10873–10882. 10.1063/1.467837.
[46] Bell, M., Hester, H.G., Gallman, A.N., Gomez, V., Pribyl, J., Rojas, G., Riegger, A., Weil, T., Watanabe, H., Chujo, Y., et al. (2019). Bulk acyclic diene metathesis polycondensation. Macromol. Chem. Phys. *220*, 1900223. 10.1002/macp.201900223.
[47] Fokou, P.A., and Meier, M.A.R. (2010). Studying and suppressing olefin isomerization side reactions during ADMET polymerizations. Macromol. Rapid Commun. *31*, 368–373. 10.1002/marc.200900678.
[48] Hong, S.H., Sanders, D.P., Lee, C.W., and Grubbs, R.H. (2005). Prevention of undesirable isomerization during olefin metathesis. J. Am. Chem. Soc. *127*, 17160–17161. 10.1021/ja052939w.
[49] Natta, G., Pasquon, I., Zambelli, A., and Gatti, G. (1964). Dependence of the melting point of isotactic polypropylenes on their molecular weight and degree of stereospecificity of different catalytic systems. Makromol. Chem. *70*, 191–205. 10.1002/macp.1964.020700114.
[50] Peterson, J.D., Vyazovkin, S., and Wight, C.A. (2001). Kinetics of the thermal and thermo-oxidative degradation of polystyrene, polyethylene and poly(propylene). Macromol. Chem. Phys. *202*, 775–784. 10.1002/1521-3935(20010301)202:6<775::AID-MACP775>3.0.CO;2-G.
[51] Beckingham, B.S., Ho, V., and Segalman, R.A. (2014). Melting behavior of poly(3-(2′-ethyl)hexylthiophene). macromolecules *47*, 8305–8310. 10.1021/ma501915v.
[52] Androsch, R., and Wunderlich, B. (2005). The link between rigid amorphous fraction and crystal perfection in cold-crystallized poly(ethylene terephthalate). Polymer *46*, 12556–12566. 10.1016/j.polymer.2005.10.099.
[53] Xu, H., and Cebe, P. (2004). Heat capacity study of isotactic polystyrene: Dual reversible crystal melting and relaxation of rigid amorphous fraction. Macromolecules *37*, 2797–2806. 10.1021/ma035961n.
[54] Wei, Z., Song, P., Zhou, C., Chen, G., Chang, Y., Li, J., Zhang, W., and Liang, J. (2013). Insight into the annealing peak and microstructural changes of poly(L-lactic acid) by annealing at elevated temperatures. Polymer *54*, 3377–3384. 10.1016/j.polymer.2013.04.027.
[55] Abiad, M.G., Campanella, O.H., and Carvajal, M.T. (2010). Assessment of thermal transitions by dynamic mechanical analysis (DMA) using a novel disposable powder holder. Pharmaceutics *2*, 78–90. 10.3390/pharmaceutics2020078.
[56] Grub, J., and Löser, E. (2011). Butadiene. In Ullmann's Encyclopedia of Industrial Chemistry (John Wiley & Sons, Ltd). 10.1002/14356007.a04_431.pub2.

Figure 1. Expanding the space of chemically recyclable hydrocarbon polymers using ADMET as a strategy for the reversible polymerization of butadiene-derived oligomers.
(A) Next-generation polymers designed for chemical recycling.
(B) Recent example of a chemically recyclable hydrocarbon polymer system.
(C) Previous work: Fe-catalyzed [2+2] cycloaddition-oligomerization of butadiene.
(D) This work: ADMET as a strategy for reversible chain-extension of DVOCB to pDVOCB.

Figure 2. Synthesis of short-chain DVOCB.
[a]Within $n \pm 0.3$ where n is determined by integration of the ^{1}H NMR spectra in $CDCl_3$ at 25°C.

Figure 3. Thermal analysis for a series of DVOCB oligomers.
(A) Overlaid TGA traces with ramp rate of 10°C/min.
(B) Overlaid DSC traces (second heating) with ramp rate of 5°C/min.

Figure 4. ADMET polymerization of DVOCB.
[a]Measured by ^{1}H NMR spectroscopy at 140°C in TCE-d_2.
[b]Measured by HT-GPC at 145°C in TCB, elution times relative to linear polyethylene.
[c]Not soluble under HT-GPC conditions.

Figure 5. Thermal analysis for a series of pDVOCB polymers.
(A) Overlaid TGA traces with ramp rate of 20°C/min.
(B) Overlaid DSC traces (second heating) with ramp rate of 5°C/min.

Figure 6. WAXS comparison of oligomer and polymer.
Variable temperature WAXS of melt-pressed samples of DVOCB(10) (A) and pDVOCB(6, 42) (B) at a temperature sweep of 5°C/min under heating. Sample temperature was calibrated using diphenylacetic acid (see also Figures S25 and S26)

Figure 7. Mechanical Properties of pDVOCB.
(A) DMA of pDVOCB(5,40), iPP (M_w = 243 kg/mol), and HDPE (M_w = 66 kg/mol) melt-pressed bars with temperature sweeps held at constant amplitude and frequency and with a heating rate of 3°C/min (see also Figure S56).
(B) Selected stress-strain curves for pDVOCB(5, 40) and pDVOCB(5, 67) melt-pressed bars.
(C) Selected stress-strain curves for low and high molecular weight iPP and HDPE melt-pressed dog-bones.

Figure 8. Chemical recycling of pDVOCB(n, m).
(A) Optimized ADMET depolymerization and repolymerization. Equivalents and mol % are relative to DVOCB units.
(B) ^{1}H NMR spectra for one cycle of chemical recycling in TCE-d_2 (6.00 ppm) at 140°C.
(C) Thermal behavior of virgin and recycled pDVOCB. Overlaid TGA traces with ramp rate of 20°C/min (top) and overlaid DSC traces (second heating) with ramp rate of 5°C/min (bottom).
(D) Chemical recycling from mixed polymer waste using the same experimental conditions as in part A.

Figure 9. Chemical recycling of DVOCB to butadiene and 1,3-divinylcyclobutane.
Yields are determined by ^{1}H NMR integration relative to an internal standard.

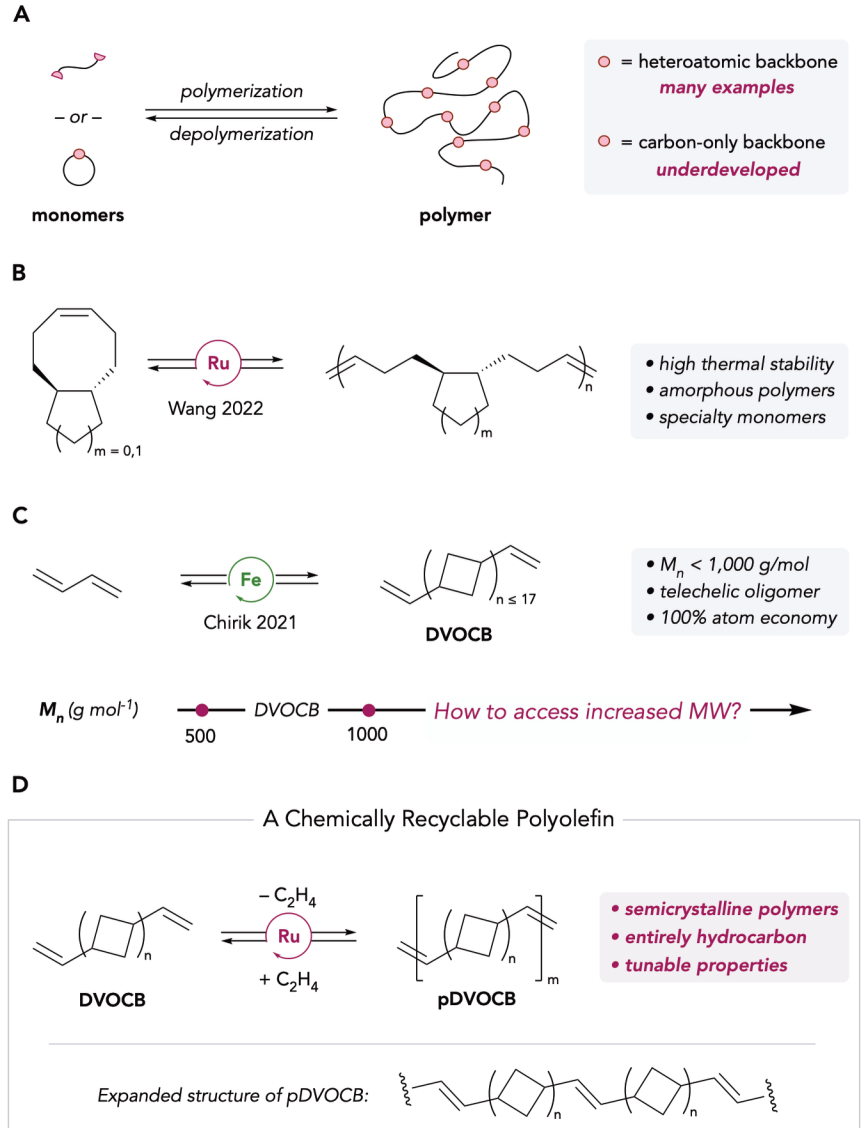
A
– or –
polymerization
depolymerization
monomers
polymer
= heteroatomic backbone
many examples
= carbon-only backbone
underdeveloped
B
m = 0,1
Ru
Wang 2022
n
m
• high thermal stability
• amorphous polymers
• specialty monomers
C
Fe
Chirik 2021
n ≤ 17
DVOCB
• Mn < 1,000 g/mol
• telechelic oligomer
• 100% atom economy
Mn (g mol-1)
500
DVOCB
1000
How to access increased MW?
D
A Chemically Recyclable Polyolefin
– C2H4
Ru
+ C2H4
n
m
DVOCB
pDVOCB
• semicrystalline polymers
• entirely hydrocarbon
• tunable properties
Expanded structure of pDVOCB:

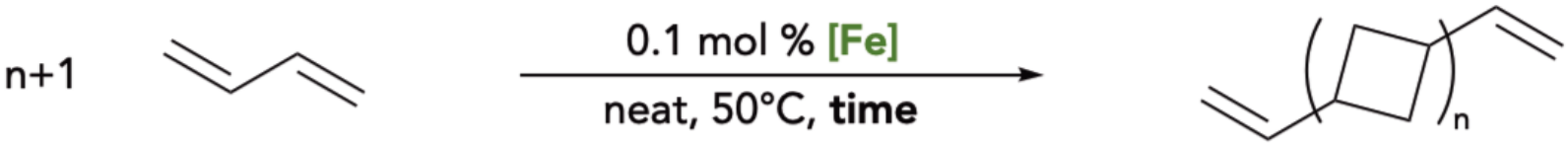

Time (h)	n^a	Yield (%)	Đ
16	4	12	1.05
22	5	25	1.05
24	6	35	1.04
28	7	44	1.03

>72% combined yield upon recycling unreacted butadiene

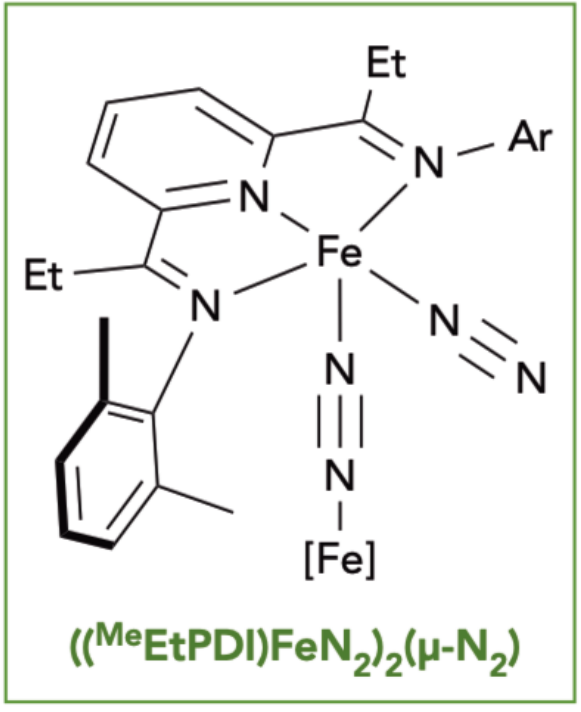

((^{Me}EtPDI)FeN_2)$_2$(μ-N_2)

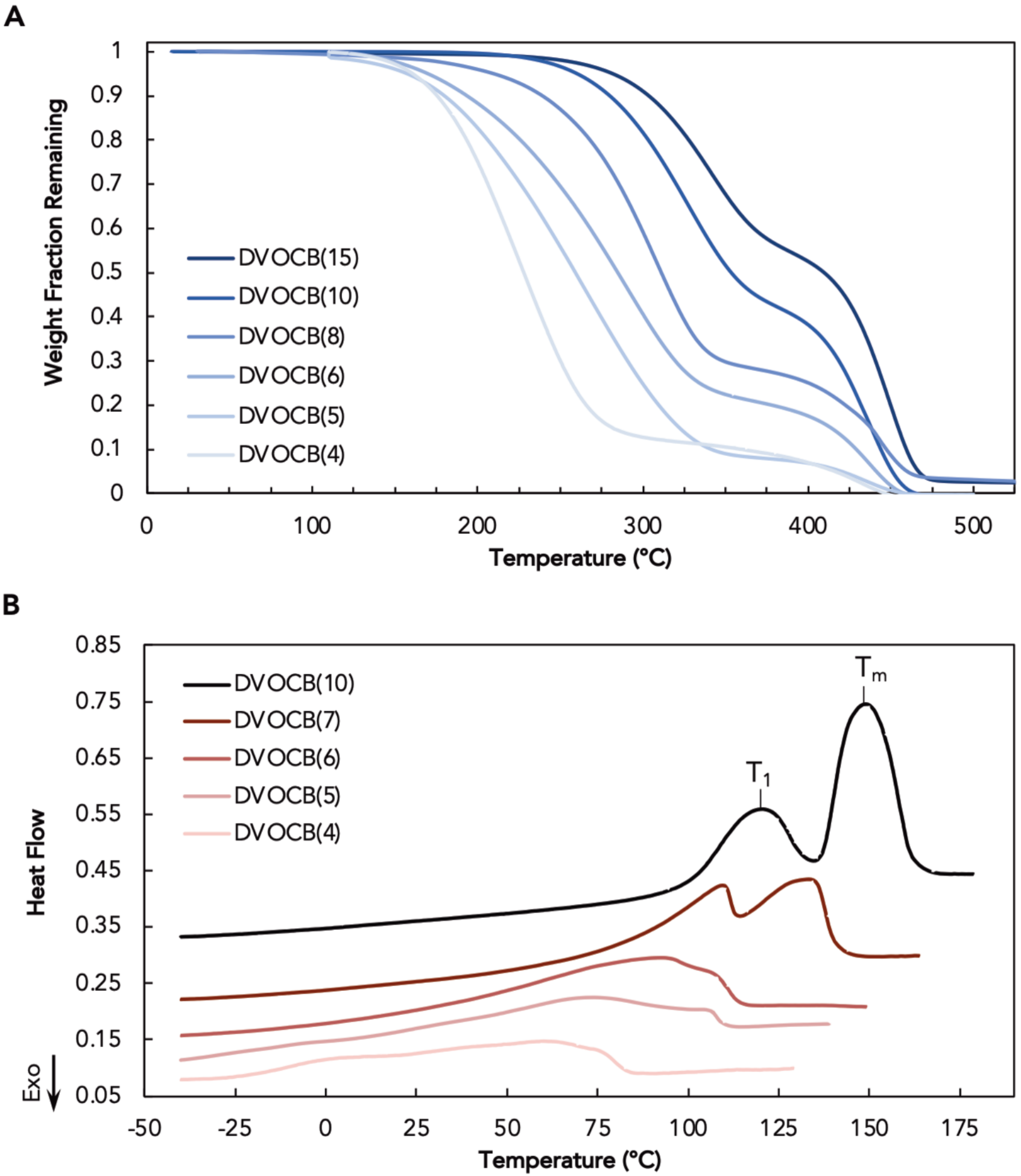
A
Weight Fraction Remaining
1
0.9
0.8
0.7
0.6
0.5
0.4
0.3
0.2
0.1
0
DVOCB(15)
DVOCB(10)
DVOCB(8)
DVOCB(6)
DVOCB(5)
DVOCB(4)
0
100
200
300
400
500
Temperature (°C)
B
Heat Flow
0.85
0.75
0.65
0.55
0.45
0.35
0.25
0.15
0.05
Exo
DVOCB(10)
DVOCB(7)
DVOCB(6)
DVOCB(5)
DVOCB(4)
T1
Tm
-50
-25
0
25
50
75
100
125
150
175
Temperature (°C)

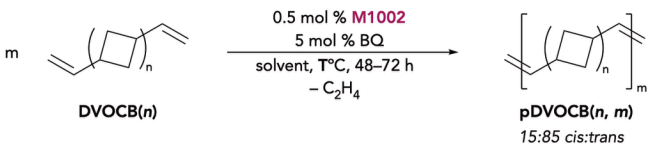

DVOCB(*n*)

pDVOCB(*n*, *m*)
15:85 cis:trans

n	*m*[a]	T (°C)	M_n (kg/mol)[a]	M_w (kg/mol)[b]	Đ[b]	Yield (%)
4	172	120	41.7	31.2	2.8	94
5	67	140	19.9	26.8	3.7	76
6	42	155	14.8	17.5	3.1	94
7	7	165	3.0	[c]	[c]	89
10	8	170	4.5	[c]	[c]	94

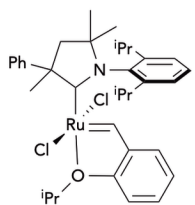

M1002

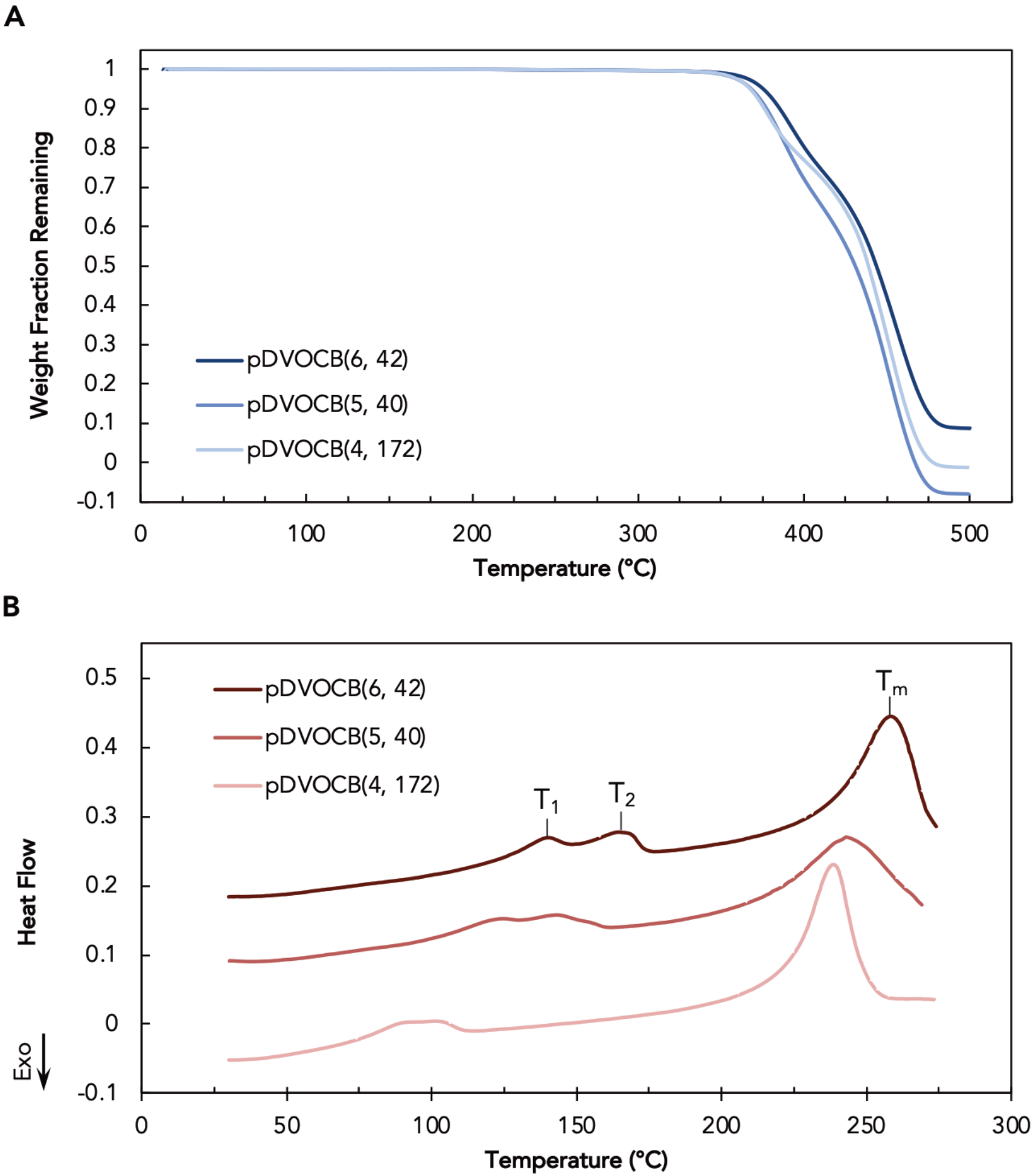
A
Weight Fraction Remaining
1
0.9
0.8
0.7
0.6
0.5
0.4
0.3
0.2
0.1
0
-0.1
pDVOCB(6, 42)
pDVOCB(5, 40)
pDVOCB(4, 172)
0
100
200
300
400
500
Temperature (°C)
B
Heat Flow
Exo
0.5
0.4
0.3
0.2
0.1
0
-0.1
pDVOCB(6, 42)
pDVOCB(5, 40)
pDVOCB(4, 172)
T1
T2
Tm
0
50
100
150
200
250
300
Temperature (°C)

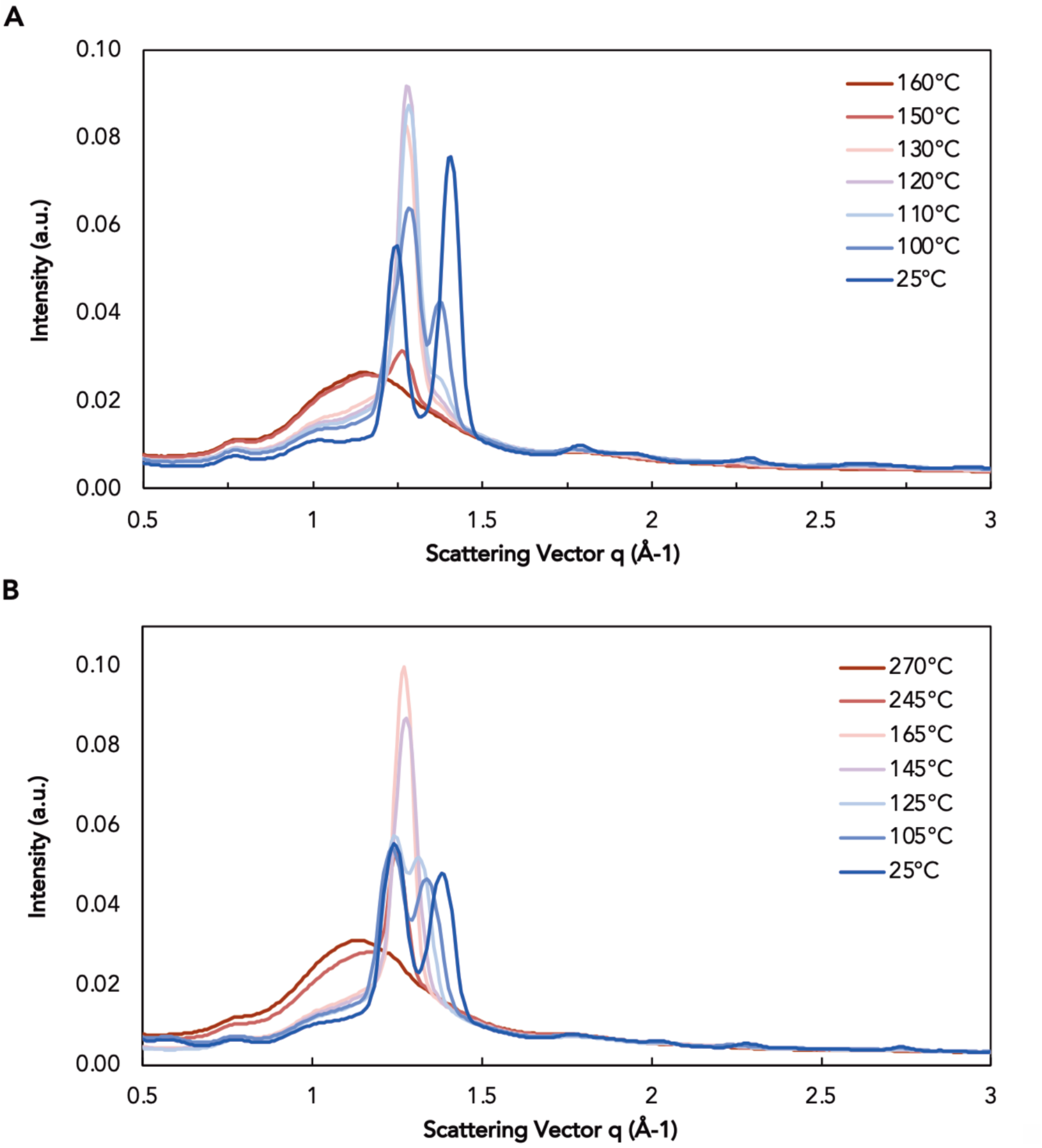
A
0.10
0.08
0.06
0.04
0.02
0.00
Intensity (a.u.)
160°C
150°C
130°C
120°C
110°C
100°C
25°C
0.5
1
1.5
2
2.5
3
Scattering Vector q (Å-1)
B
0.10
0.08
0.06
0.04
0.02
0.00
Intensity (a.u.)
270°C
245°C
165°C
145°C
125°C
105°C
25°C
0.5
1
1.5
2
2.5
3
Scattering Vector q (Å-1)

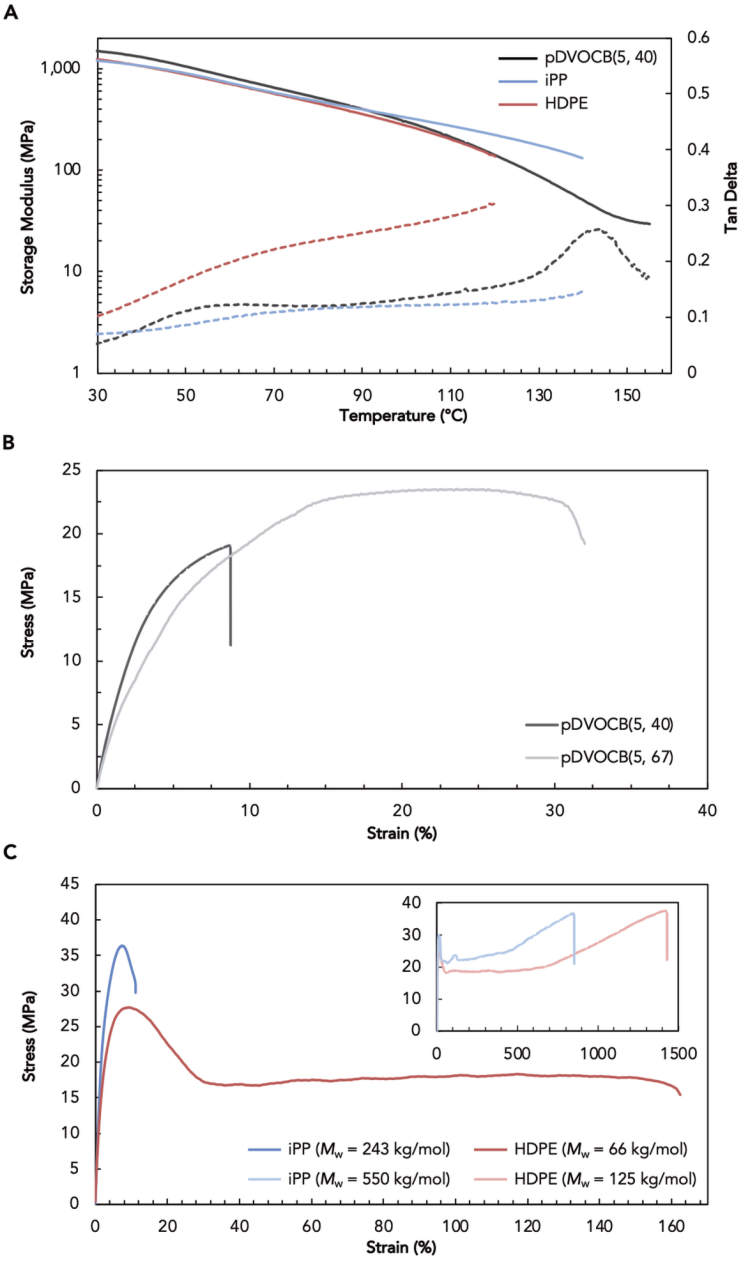
A
Storage Modulus (MPa)
Tan Delta
Temperature (°C)
pDVOCB(5, 40)
iPP
HDPE
B
Stress (MPa)
Strain (%)
pDVOCB(5, 40)
pDVOCB(5, 67)
C
Stress (MPa)
Strain (%)
iPP (Mw = 243 kg/mol)
iPP (Mw = 550 kg/mol)
HDPE (Mw = 66 kg/mol)
HDPE (Mw = 125 kg/mol)

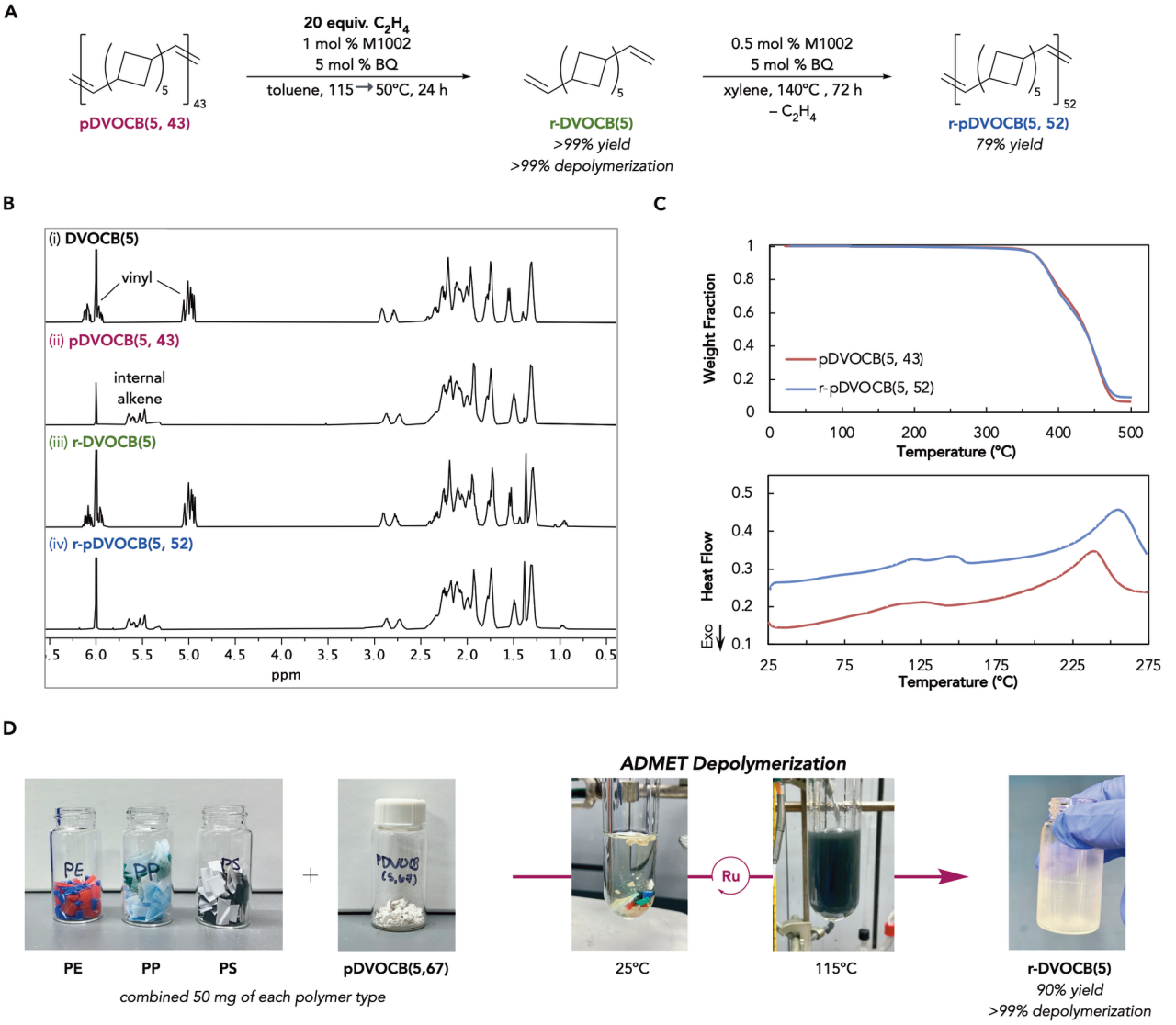
A
20 equiv. C2H4
1 mol % M1002
5 mol % BQ
toluene, 115→50°C, 24 h
pDVOCB(5, 43)
r-DVOCB(5)
>99% yield
>99% depolymerization
0.5 mol % M1002
5 mol % BQ
xylene, 140°C , 72 h
– C2H4
r-pDVOCB(5, 52)
79% yield
B
(i) DVOCB(5)
vinyl
(ii) pDVOCB(5, 43)
internal
alkene
(iii) r-DVOCB(5)
(iv) r-pDVOCB(5, 52)
ppm
C
Weight Fraction
pDVOCB(5, 43)
r-pDVOCB(5, 52)
Temperature (°C)
Heat Flow
Exo
Temperature (°C)
D
ADMET Depolymerization
PE
PP
PS
pDVOCB(5,67)
combined 50 mg of each polymer type
Ru
25°C
115°C
r-DVOCB(5)
90% yield
>99% depolymerization

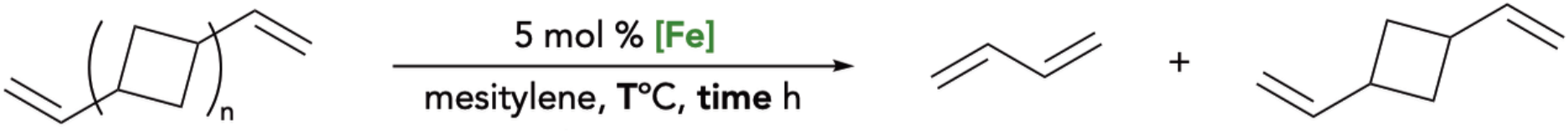

DVOCB(*n*) **BD** **DVCB**

Oligomer	**T** (°C)	**Time** (h)	**BD** (%)	**DVCB** (%)	**Total Volatiles** (%)
DVOCB(6)	50	16	5	<1	5
DVOCB(6)	70	16	15	4	19
DVOCB(6)	90	16	63	13	76
r-DVOCB(5)	90	24	79	21	>99

A Recyclable Polyolefin From Butadiene

monomer

commodity feedstock

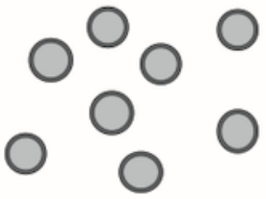

=

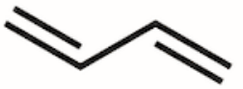

[2+2]

oligomer

tunable properties

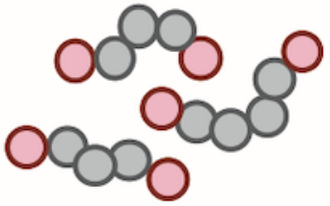

=

ADMET

polymer

semicrystalline morphology

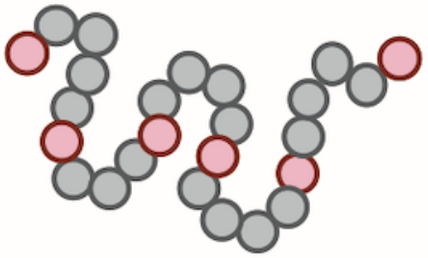

=